Channel Reciprocity Calibration for Hybrid Beamforming in Distributed MIMO Systems

Nariman Torkzaban
University of Maryland, College Park
College Park, MD
narimant@umd.edu

Mohammad A. (Amir) Khojastepour NEC Laboratories, America Princeton, NJ amir@nec-labs.com

John S. Baras
University of Maryland, College Park
College Park, MD
baras@umd.edu

Abstract—Time Division Duplex (TDD)-based distributed massive MIMO systems are envisioned as candidate solution for the physical layer of 6G multi-antenna systems supporting cooperative hybrid beamforming that heavily relies on the obtained uplink channel estimates for efficient coherent downlink precoding. However, due to the hardware impairment between the transmitter and the receiver, full channel reciprocity does not hold between the downlink and uplink direction. Such reciprocity mismatch deteriorates the performance of mm-Wave hybrid beamforming and has to be estimated and compensated for, to avoid performance degradation in the co-operative hybrid beamforming.

In this paper, we address the channel reciprocity calibration between any two nodes at two levels. We decompose the problem into two sub-problems. In the first sub-problem, we calibrate the digital chain, i.e. obtain the mismatch coefficients of the (DAC/ADC) up to a constant scaling factor. In the second sub-problem, we obtain the (PA/LNA) mismatch coefficients. At each step, we formulate the channel reciprocity calibration as a least-square optimization problem that can efficiently be solved via conventional methods such as alternative optimization with high accuracy. Finally, we verify the performance of our channel reciprocity calibration approach through extensive numerical experiments.

Index Terms—Hybrid Beamforming, Distributed MIMO, Channel Reciprocity, Reciprocity Calibration.

I. Introduction

Massive MIMO is considered as an enabling technology towards realizing 5G and beyond communications, since the large number of antennas per base station allows for extended coverage, effective beamforming [1][2], higher data rates per users [3], and better spectral efficiency [4]. However, such network densification technique contributes to the inter-cell-interference (ICI) effect which negatively impacts the performance of the wireless communications system. To overcome this issue, the concept of distributed massive MIMO systems is envisioned as a potential technology for realizing 6G multi-antenna systems [5].

A distributed massive MIMO system is a scalable[3] implementation of coordinated multi-point transmission (CoMP), where a multitude of access points (APs) that are geographically separated, co-operate towards jointly serving the mobile users (MUs) with the goal of increasing the received signal quality and system throughput [6]. Each AP has its own local oscillator and may possibly employ a large array of antennas. The APs are interconnected and connected to a

central server (CS) through wired backhauling (e.g. Ethernet). To enable beamforming to a user in the downlink the nodes which are involved in the downlink transmission need to know the downlink channel to a particular user. To avoid feedback overhead, the AP may be able to estimate the downlink channel if the downlink and uplink are at the same frequency. Therefore, the recommended scheme for distributed MIMO systems is time-division duplex (TDD).

Under the TDD scheme, each AP is enabled to estimate the uplink channel using the uplink pilot symbols received from the user equipments (UEs). Exploiting the reciprocity of the UL-DL channel, the uplink estimates can be utilized for estimating the downlink channel. This is typically termed as a reciprocitybased channel estimation in the literature. Under ideal channel reciprocity, once the uplink channel is estimated the same estimate can be used as the equivalent for the downlink channel. However, in practice full channel reciprocity does not hold in general due to the non-reciprocity in the RF chains of the transceivers at the channel end-points. To overcome this issue, calibration techniques must be used to tune the transceivers hardware for reciprocity-based channel estimation to become feasible. Several types of signaling exist in the literature for reciprocity calibration. A line of research proposes to perform calibration utilizing the bidirectional channel between the APs and the UEs[7]. Some other approaches perform internal calibration at the APs[8][9], while some works consider overthe-air signaling between the APs. Given that bidirectional signaling between the APs and the UEs highly depends on the quality of the UEs links and that deploying cables for the sake of calibration between the distributed APs is not practical, it is widely supported that the third calibration approach is the right solution for distributed MIMO systems [5][10][11].

Fig. 1 depicts the structure of a hybrid beamformer. Regardless of the imperfection in the phase shifter network (PSN), the reciprocity mismatch at hybrid beamforming systems, stems from the imperfection in the hardware at the *digital* and the *analog* RF chains. More precisely, at the digital RF chain, the digital-to-analog converter and analog-to-digital converter (DAC/ADC), and at the analog chain, the power amplifier and the low-noise amplifier (PA/LNA) require calibration for channel reciprocity. Therefore, although the literature on reciprocity calibration for fully-digital beamforming is rich, reciprocity

mismatch in hybrid beamforming systems need to be addressed differently. Reciprocity calibration for hybrid beamforming in TDD-based massive MIMO systems was first addressed in [12], where the authors used an internal calibration method where they considered a PSN with sub-array based architecture. As opposed to this pioneer work, and similar to [13][5][4], in this paper we considered a fully-connected PSN. Within the context of distributed massive MIMO systems, the authors in [5] proposed a maximum likelihood (ML)-based calibration relying on joint beam sweep by all APs in the network. The authors consider a single mismatch parameter per AP and only consider fully-digital beamforming. As opposed to this work, in this paper we consider a single mismatch coefficient per digital RF chain which allows for a much more precise reciprocity calibration. However, among the prior art, at the macroscopic level our approach remains closest to the one presented in [14] where the authors decompose the channel reciprocity calibration in TDD hybrid beamforming systems into two disjoint problems. They first come up with a closedform solution for the calibration of the digital chain and then formulate and solve an optimization problem to calibrate the analog chain. In [13] calibration of the PSN is considered. Having taken this imperfection into account in a later work, the authors calibrate the analog and digital chain in the hybrid massive MIMO system[4]. In this paper, we decompose the channel reciprocity calibration task for hybrid beamforming into two sub-problems. The first sub-problem entails calibrating the the digital chain up to an unknown scaling factor. Having obtained the calibration parameters of the digital chain, the second sub-problem aims at calibrating the analog RF chain. We note that compared to the prior art, our approach has minimal overhead in terms of the number of communication rounds required for estimating the calibration parameters.

The remainder of the paper is organized as follows. Section II describes the system model. In Section III we describe our proposed method for reciprocity calibration between two arbitrary nodes. Section IV presents our evaluation results, and finally, in Section V, we highlight our conclusions.

II. SYSTEM MODEL

We consider a distributed mmWave MIMO system where a cluster of co-operative multi-antenna APs employing hybrid beamforming, jointly serve mobile users (MUs).

A. Beamforming Model

The hybrid beamformer comprises of a first level digital beamformer and a second level analog beamformer. Each AP is equipped with $N_{\rm ap}$ digital RF chains which are fed by the output of the digital beamformer for each transmitted streams. In turn, the output of the digital RF chain goes through an analog beamformer which is connected to $M_{\rm ap}$ analog RF chains each of which connected to an antenna element where the antenna elements are arranged in a uniform linear array (ULA) structure. The analog beamformers are usually comprised of phase-only vectors which are implemented by fully-connected phase shift network (PSN) [4] between the output of the digital

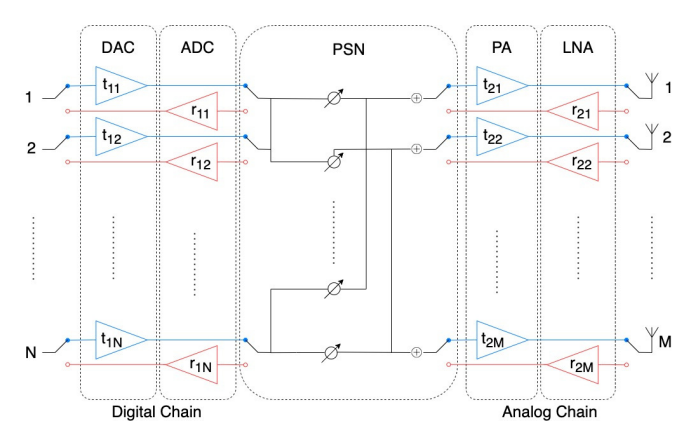


Fig. 1: Hybrid Beamforming System Model

RF chains and input of the analog RF chains. In a subarray-based structure [12] the output of each digital RF chain feeds a disjoint set of analog RF chains (or antennas), hence, the analog beamformer has a block diagonal structure. We consider a general analog beamformer in this paper (except for a practical constraint discussed later in Section III) that can treat either of the fully-connected or subarray-based structures as an special case. At the MUs, there are $M_{\rm mu}$ and $N_{\rm mu}$ analog and digital RF chains, respectively.

B. Channel Model

The mmWave channel between each AP and each MU is assumed to have only a few spatial clusters $L \ll N_{\rm ap}, N_{\rm mu}$, where L is the number of scatterers, determining the number of paths between each AP and each MU. We consider a geometric channel model that is given by,

$$\mathbf{H} = \sqrt{\frac{N_{\rm ap}N_{\rm mu}}{L}} \sum_{\ell=1}^{L} \alpha_{\ell} \mathbf{a}_{\rm mu} \left(\phi_{\ell}\right) \mathbf{a}_{\rm ap}^{T} \left(\theta_{\ell}\right) \tag{1}$$

where $\alpha_l \sim \mathcal{CN}\left(0,\sigma_{\alpha}^2\right)$ is the gain of the l-th path, $\mathbf{a}_{\mathrm{mu}}\left(\phi_{\ell}\right) \in \mathbb{C}^{N_{\mathrm{mu}}}$, and $\boldsymbol{a}_{\mathrm{ap}}\left(\theta_{\ell}\right) \in \mathbb{C}^{N_{\mathrm{ap}}}$ denote the directivity vectors of the MUs and the APs at the angles of arrival (AoA) $\phi_{\ell} \in [-\pi/2,\pi/2)$ to the MUs, and the angles of departure (AoD) $\theta_{\ell} \in [-\pi/2,\pi/2)$ from the APs. The directivity vectors $\boldsymbol{a}_{\mathrm{ap}}$, and $\boldsymbol{a}_{\mathrm{mu}}$ are given by,

$$\mathbf{a}_{ap}(\theta_{\ell}) = \left[1, e^{-j\frac{2\pi d}{\lambda}\sin\theta_{\ell}}, \cdots, e^{-j\frac{2\pi d}{\lambda}(N_{ap}-1)\sin\theta_{\ell}}\right]^{T},$$

$$\mathbf{a}_{mu}(\phi_{\ell}) = \left[1, e^{-j\frac{2\pi d}{\lambda}\sin\phi_{\ell}}, \cdots, e^{-j\frac{2\pi d}{\lambda}(N_{mu}-1)\sin\phi_{\ell}}\right]^{T}, \quad (2)$$

where λ is the carrier wavelength and d denotes the distance between every two adjacent antenna elements and is set as $d=\lambda/2$. The effective channel between any AP and MU is a function of the mmWave channel and the transfer functions of the RF chains, the PSNs, and the analog beamformers on both sides. The uplink (UL) and the downlink (DL) channels are give by,

$$\mathbf{H}_{DL} = \mathbf{R}_{\text{mu},1} \mathbf{B}^T \mathbf{R}_{\text{mu},2} \mathbf{H} \mathbf{T}_{\text{ap},2} \mathbf{F} \mathbf{T}_{\text{ap},1}, \tag{3}$$

$$\mathbf{H}_{UL} = \mathbf{R}_{\mathrm{ap},1} \mathbf{F}^T \mathbf{R}_{\mathrm{ap},2} \mathbf{H}^T \mathbf{T}_{\mathrm{mu},2} \mathbf{B} \mathbf{T}_{\mathrm{mu},1}$$
(4)

where $\mathbf{T}_{ap,1}, \mathbf{R}_{ap,1} \in \mathbb{C}^{N_{ap} \times N_{ap}}$ are the digital reciprocity calibration matrices which denote the frequency responses of the transmit and receive digital RF chains (DAC/ADC) at the AP, $\mathbf{T}_{ap,2}, \mathbf{R}_{ap,2} \in \mathbb{C}^{M_{ap} \times M_{ap}}$ are the analog reciprocity calibration matrices which denote the transmit and receive frequency responses of the analog chains (PA/LNA) at the AP, respectively. Similarly, at the MU, $\mathbf{T}_{\text{mu},1}, \mathbf{R}_{\text{mu},1} \in \mathbb{C}^{N_{\text{mu}} \times N_{\text{mu}}}$ denote the frequency responses of the transmit and receive digital RF chains, and $\hat{\mathbf{T}}_{\text{mu},2}, \mathbf{R}_{\text{mu},2} \in \mathbb{C}^{M_{\text{mu}} \times M_{\text{mu}}}$ are the transmit and receive frequency responses of the analog chain. We note that all these matrices are diagonal with the diagonal elements modeling the gain and phase characteristics of each of the chain elements. The off-diagonal entries model the cross-talk between the RF hardware that is assumed to be almost zero under proper RF design [15]. We assume that all the transceivers store codebooks for the hybrid beamforming task where each codebook consists of codewords that each represent a beamforming vector. The $\mathbf{F} \in \mathbb{C}^{M_{\mathrm{ap}} \times N_{\mathrm{ap}}}$ and $\mathbf{B} \in \mathbb{C}^{M_{\mathrm{mu}} \times N_{\mathrm{mu}}}$ are known the beamforming matrices at the AP and the MU, respectively where each beamforming matrix consists of N_t beamforming vectors. The matrices **B** and **F** model the beamformers that precode the input analog streams that are then amplified and sent to to the analog chains. We note that each AP or MU use the same matrices for beamforming both when transmitting and receiving. The transmission in the DL direction can be modeled by,

$$\mathbf{y}_{DL} = \mathbf{H}_{DL} \mathbf{x}_{DL} + \mathbf{z}_{DL} \tag{5}$$

$$\mathbf{y}_{UL} = \mathbf{H}_{UL}\mathbf{x}_{UL} + \mathbf{z}_{UL} \tag{6}$$

where $\mathbf{x}_{\mathrm{DL}} \in \mathbb{C}^{N_{\mathrm{ap}}}$ and $\mathbf{x}_{\mathrm{UL}} \in \mathbb{C}^{N_{\mathrm{mu}}}$ are the input streams to the digital RF chains (i.e., the output of the baseband processing unit (BBU) which could in turn be digitally precoded symbols) the AP and the MU, respectively. In the DL direction, the AP may use a digital precoder $\mathbf{W} \in \mathbb{C}^{N_{\mathrm{ap}} \times N_s}$, such that $\mathbf{x}_{\mathrm{DL}} = \mathbf{W}\mathbf{s}$ where $\mathbf{s} \in \mathbb{C}^{N_s}$ is the vector of digital symbols transmitted from the AP with $N_s \leq N_{\mathrm{ap}}$ being the number of data streams, $\mathbf{y}_{\mathrm{DL}} \in \mathbb{C}^{M_{\mathrm{mu}}}$ and $\mathbf{y}_{\mathrm{UL}} \in \mathbb{C}^{M_{\mathrm{ap}}}$ are the vectors of the received signal streams at the BBU in the DL and UL directions, respectively, and $\mathbf{z}_{\mathrm{DL}} \in \mathbb{C}^{M_{\mathrm{mu}}}$ and $\mathbf{z}_{\mathrm{UL}} \in \mathbb{C}^{M_{\mathrm{ap}}}$ are the vectors of the additive white Gaussian noise (AWGN) with the distributions $\mathbf{z}_{\mathrm{DL}} \sim \mathcal{CN}\left(\mathbf{0}, \sigma_z^2 \mathbf{I}_{M_{\mathrm{mu}}}\right)$ and $\mathbf{z}_{\mathrm{UL}} \sim \mathcal{CN}\left(\mathbf{0}, \sigma_z^2 \mathbf{I}_{M_{\mathrm{np}}}\right)$.

III. RECIPROCITY CALIBRATION BETWEEN TWO NODES

In this section, we address calibration between two nodes S and S'. Without loss of generality we assume each node employs M analog RF chains and N digital RF chains. The goal is to estimate a combination of the digital and analog calibration matrices in the transmit and receive paths for both nodes in such a way that the channel estimation in one direction can be used in the reverse direction. To this end, we propose a two-step approach for calibration process where in the first step we estimate the digital reciprocity calibration matrices and in the second step we estimate a combination of the analog reciprocity matrices. As becomes evident in the following, there is no sub-optimality in breaking the calibration

process into two steps, and our approach takes advantage of the estimated parameters in the first step in the second step in order to minimize the number of pilot transmission required for calibration. This is in fact very important to minimize the time spent on calibration not only to reduce the calibration overhead but also to make sure that the channel variation is negligible during the calibration process.

In the first step, the digital reciprocity calibration matrices in the transmit and receive paths for either of the nodes are estimated up to a scaling factor. Without loss of generality, as we will discuss later, we use the calibration parameter corresponding to the first antenna element as the scaling factor. In the second step, we use the estimation of the digital calibration matrices in formulating the problem of finding a combination of analog calibration matrices that are required to benefit from channel reciprocity. Although no claim of optimality is made, the proposed approach is built on a particular pilot transmission and analog beamformer selection with the aim of minimizing the number of transmissions required to perform the reciprocity calibration. This is particularly important due to the fact that during the transmission of a group of such pilots the channel variation is assumed to be negligible. Moreover, reciprocity calibration has to be performed periodically in order to capture the effect of variation in the properties of the elements in the analog and digital RF chains. Hence, an efficient calibration process with minimum possible time should be devised in order to reduce the overhead of the calibration.

It is important to note that even during pilot transmissions, hybrid beamforming is employed by using proper analog beamformers (i.e., transmit and receive beamformers). A proper analog beamformer usually uses the entire transmit antenna array, i.e., the weight corresponding to each antenna element is nonzero. This property trivially holds in the special case that the analog beamformers are implemented by a PSN. This property is important in practice to ensure good beamforming gain, as in theory one may suggest to use a trivial beamformer which activates only one antenna in order to expedite the calibration process to a linear time based on the number of antennas. Although in an abstract theoretical analysis, such beamformers may seem to be the most efficient in terms of reducing the calibration time, in practice, an analog beamformer which uses a single antenna in average transmits (or receives) a fraction of 1/M power in comparison to a beamformer which uses the entire antenna array that consist of M antenna elements. As a result of this important practical limitation on the analog beamformers, we will see that even though the first step, i.e., the digital chain reciprocity calibration, may be performed in linear time with respect to the number of digital RF chains, the second step, i.e., the analog chain reciprocity calibration between two nodes, requires quadratic time with respect to the number of analog RF chains, i.e., number of antenna elements.

A. Digital Chain Reciprocity Calibration

In order to estimate the digital transmit matrix \mathbf{T}_1 at node S and digital receive matrix \mathbf{R}_1' at node S', we transmit N consecutive pilot signals from N different digital RF chains

of node S with the digital reciprocity calibration parameters $t_{1i}, i=1,\ldots,N$. In all these transmissions, we use an arbitrary but unique beamforming vector, say \mathbf{f}_1 . In other words, we use the pilot signal $\mathbf{s}=[s]$ and $\mathbf{F}=\mathbf{f}_1$ in (6). On the receiver side, the node S' will receive on all its digital RF chains using the $M\times N$ receive beamforming matrix \mathbf{B} that is defined as $\mathbf{B}=[\mathbf{b}_1,\mathbf{b}_1,\ldots,\mathbf{b}_1]$, i.e., consisting of N column vectors b_1 . The received signal for the i-th transmission is given by

$$\mathbf{y}_{i}' = \mathbf{R}_{1}' \mathbf{B}^{T} \mathbf{R}_{2}' \mathbf{H} \mathbf{T}_{2} \mathbf{f}_{1} t_{1i} s + z_{DL}, \quad \forall i = 1 \dots N$$
 (7)

where \mathbf{R}_1' is a diagonal matrix with the diagonal elements with the diagonal elements $r_{1i}', i=1,\ldots,N$ represented by the vector $\mathbf{r}_1'=[r_{11}',\ldots,r_{1N}']$. Similarly, for the diagonal matrix \mathbf{T}_1 , \mathbf{T}_2 , and \mathbf{R}_2' we define $\mathbf{t}_1=[t_{11},\ldots,t_{1N}]$, $\mathbf{t}_2=[t_{21},\ldots,t_{2N}]$, and $\mathbf{r}_2'=[r_{21}',\ldots,r_{2N}']$. Further, define the scaling factor $h\doteq \mathbf{b}_1^T\mathbf{R}_2'\mathbf{H}\mathbf{T}_2\mathbf{f}_1$. Therefore, $\mathbf{R}_1'\mathbf{B}^T\mathbf{R}_2'\mathbf{H}\mathbf{T}_2\mathbf{f}_1t_{1i}$ can be estimated from (7) as,

$$\tilde{\mathbf{y}}_i' = \mathbf{R}_1' h t_{1i}, \quad \forall i = 1 \dots N$$
 (8)

Note that for all $k,l \in 1..N$, the relation between any r'_{1k} and r'_{1l} can be easily found as $r'_{1k}/r'_{1l} = \tilde{y}'_{ik}/\tilde{y}'_{il}$ through any of the N equations in (8) where \tilde{y}'_{ik} is the k-th element of the vector $\tilde{\mathbf{y}}'$. Therefore, the \mathbf{R}'_1 matrix can be estimated up to a scaling factor. However, there are N such noisy observations that may each result in different noisy estimates for \mathbf{R}'_1 . Similar argument goes for \mathbf{T}_1 . To get a more reliable estimate of both \mathbf{R}'_1 and \mathbf{T}_1 , we formulate the following optimization problem in order to find first level reciprocity calibration matrices.

Problem 1. (First-level Reciprocity Calibration)

The transmit and receive matrices \mathbf{T}_1 , and \mathbf{R}'_1 can be found up to a scaling factor as the solution to the following least-square minimization problem.

$$\mathbf{T}_{1}, \mathbf{R}'_{1} = \arg\min \sum_{i=1}^{N} \sum_{j=1}^{N} \|y'_{ij} - r'_{1i}ht_{1j}\|^{2}$$
(9)

Solving Problem 1, enables us to estimate the digital transmit matrix \mathbf{T}_1 at node S and digital receive matrix \mathbf{R}_1' at node S' with N^2 observations that are achieved through only N transmissions. Similarly, the digital transmit matrix \mathbf{T}_1' at node S' and digital receive matrix \mathbf{R}_1 at node S can also be determined with additional N pilot transmission from node S' that results in additional N^2 observations.

B. Analog Chain Reciprocity Calibration

Having determined the \mathbf{R}_1 , \mathbf{T}_1 , \mathbf{R}'_1 , \mathbf{T}'_1 matrices up to an unknown scaling factor, in this section, we focus on estimating the receive and transmit matrices of the analog chain. In order to do so, we perform an structured pilot transmission over different digital transmit chains and for each such transmission we receive on all N digital receive chains as described in the following. We select M transmit beamformer \mathbf{f}_i , $i = 1, \ldots, M$ and \mathbf{b}_i , $i = 1, \ldots, M$ from the transmit and receive codebook, respectively, such that the matrices $\mathbf{F} = [\mathbf{f}_1, \mathbf{f}_2, \ldots, \mathbf{f}_M]$ and

 $\mathbf{B} = [\mathbf{b}_1, \mathbf{b}_2, \dots, \mathbf{b}_M]$ are full rank. For each \mathbf{f}_i , $i = 1, \dots, M$, we perform $k = 0, 1, \dots, \lceil M/N \rceil - 1$ transmissions with transmit beamformer \mathbf{f}_i from chain 1, and receive beamformers $\mathbf{b}_{1+kN}, \mathbf{b}_{2+kN}, \dots, \mathbf{b}_{N+kN}$ for the k^{th} transmission with the beamformer \mathbf{f}_i , where $\mathbf{b}_m = \mathbf{b}_1$ for m > M. Hence, after $M \lceil M/N \rceil$ transmission we gather M^2 observations that we arrange in a $M \times M$ matrix \mathbf{Y} . Using the model in the downlink direction (6), we can write

$$\mathbf{y}'_{ki} = \mathbf{R}'_1 \mathbf{B}_k^T \mathbf{R}'_2 \mathbf{H} \mathbf{T}_2 \mathbf{f}_i t_{11} s + \mathbf{z}'_{ki}, \tag{10}$$

for all $k=1,\ldots,\lceil M/N \rceil$ and $i=1,\ldots,M$ where the estimated values for \mathbf{R}_1' is already computed in the last step up to an scaling factor r_{11}' . The $j^{th},\ j=1,\ldots,N$ row of the matrix product $\mathbf{R}_1'\mathbf{B}_k$ for $k=1,\ldots,\lceil M/N \rceil$ is given by a row vector $r_{1j}'\mathbf{b}_{N(k-1)+j}^T=r_{11}'(r_{1j}'/r_{11}')\mathbf{b}_{N(k-1)+j}^T=r_{11}'\tilde{\mathbf{b}}_m^T$ where m=N(k-1)+j. Stacking the these row vectors $\tilde{\mathbf{b}}_m^T$ for $m=1,\ldots,M$ results in an $M\times M$ matrix $\tilde{\mathbf{B}}$. Considering $\mathbf{F}=[\mathbf{f}_1,\mathbf{f}_2,\ldots,\mathbf{f}_M]$ which consists of all M transmit beamforming vectors and the modified received beamforming vectors in $\tilde{\mathbf{B}}$, we would get an aggregate $M\times M$ observation matrix \mathbf{Y}' as

$$\mathbf{Y}' = r'_{11}\tilde{\mathbf{B}}^T \mathbf{R}'_2 \mathbf{H} \mathbf{T}_2 \mathbf{F} t_{11} s' + \mathbf{Z}'$$
(11)

In a similar fashion, in the uplink direction we can write,

$$\mathbf{Y} = r_{11}\tilde{\mathbf{F}}^T \mathbf{R}_2 \mathbf{H}^T \mathbf{T}_2' \mathbf{B} t_{11}' s + \mathbf{Z}. \tag{12}$$

Let $\tilde{\mathbf{Y}}'$ and $\tilde{\mathbf{Y}}$ be the estimation of $r'_{11}\tilde{\mathbf{B}}^T\mathbf{R}'_2\mathbf{H}\mathbf{T}_2\mathbf{F}t_{11}$ and $r_{11}\tilde{\mathbf{F}}^T\mathbf{R}_2\mathbf{H}^T\mathbf{T}'_2\mathbf{B}t'_{11}$ based on (11) and (12), respectively. We have the following two observations for the channel,

$$\tilde{\mathbf{H}}_{1} = (r'_{11}t_{11})^{-1}\mathbf{R}'_{2}^{-1}\tilde{\mathbf{B}}^{-T}\tilde{\mathbf{Y}}'\mathbf{F}^{-1}\mathbf{T}_{2}^{-1}$$
(13)

$$\tilde{\mathbf{H}}_{2} = (r_{11}t'_{11})^{-1}\mathbf{T}_{2}^{\prime -1}\mathbf{B}^{-T}\tilde{\mathbf{Y}}^{T}\tilde{\mathbf{F}}^{-1}\mathbf{R}_{2}^{-1}$$
(14)

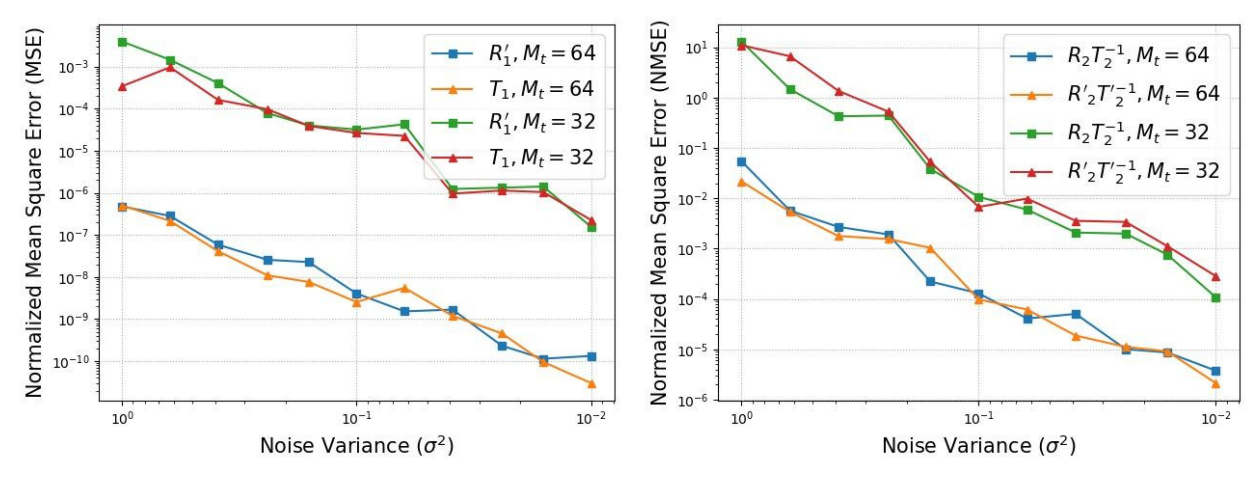
Now, define $\mathbf{X} \doteq \tilde{\mathbf{B}}^{-T} \tilde{\mathbf{Y}}' \mathbf{F}^{-1}$ and $\mathbf{Z} \doteq \mathbf{B}^{-T} \tilde{\mathbf{Y}}^T \tilde{\mathbf{F}}^{-1}$, where $\mathbf{X}, \mathbf{Z} \in \mathbb{C}^{M \times M}$ are completely known. Let x_{ij} and z_{ij} be the elements of the \mathbf{X} and \mathbf{Z} matrices for all $i, j = 1 \dots M$. We have.

$$\frac{\tilde{h}_{1,ij}}{\tilde{h}_{2,ij}} = \frac{x_{ij}r_{2i}^{\prime-1}t_{2j}^{-1}}{z_{ij}t_{2i}^{\prime-1}r_{2j}^{-1}} \cdot \frac{r_{11}^{\prime-1}t_{11}^{-1}}{t_{11}^{\prime-1}r_{11}^{-1}} \approx 1. \quad \forall i, j = 1 \dots M$$
 (15)

Let us define $\beta=r_{11}^{-1}t_{11}'^{-1}/(r_{11}'^{-1}t_{11}'^{-1})$, and $\alpha_i=r_{2i}t_{2i}^{-1}$, $\alpha_i'=r_{2i}'t_{2i}'^{-1}$. We have

$$\frac{\alpha_j}{\alpha_i'} \approx \beta \frac{z_{ij}}{x_{ij}}. \quad \forall i, j = 1...M$$
 (16)

This means that given α_1 , we can find all α_i 's and α_i' 's based on a single scaling factor that is α_1 . Please note that the product of $\mathbf{R}_2\mathbf{T}_2^{-1}$ is a diagonal matrix where the diagonal elements are given by $[\alpha_1,\alpha_2,\ldots,\alpha_M]$. Similarly, $\mathbf{R}_2'\mathbf{T}_2'^{-1}$ the follows a diagonal structure with the diagonal elements given as $[\alpha_1',\alpha_2',\ldots,\alpha_M']$. In order to minimize the estimation error, the estimation of each fraction is not performed individually and we formulate the problem as a joint least square optimization which involves all fractions in order to get the best estimates of the second-level calibration matrices as follows.



- (a) First-level Calibration Normalized MSE (NMSE)
- (b) Second-level Calibration Normalized MSE (NMSE)

Fig. 2: Normalized Reciprocity Calibration MSE.

Problem 2. (Second-level Reciprocity Calibration)

The second-level analog chain matrices can be found as the solution to the following least-square optimization problem.

$$\{\alpha_{i}, \alpha_{i}'\}_{i=1}^{M} = \arg \min_{\alpha_{i}, \alpha_{j}', i, j \in [M]} \sum_{i=1}^{M} \sum_{j=1}^{M} \|x_{ij}\alpha_{j} - \beta z_{ij}\alpha_{i}'\|^{2}$$
(17)

Having found the best estimates of α_i and α'_i parameters, the mismatch calibration matrices $\mathbf{R}_2\mathbf{T}_2^{-1}$ and $\mathbf{R}'_2\mathbf{T}'_2^{-1}$ can be easily formed and found up to a scaling factor as the second-level calibration matrices.

IV. PERFORMANCE EVALUATION

In this section, we first describe the simulation setup and then proceed to the analysis of the numerical results.

A. Simulation Setup and Parameters

We consider two nodes with $M_t=32,64$ and $M_r=32,64$ antennas and $N_t=M_t/4$, and $N_r=M_r/4$ digital RF chains, respectively. We consider a multi-path channel model with L=4 paths. We assume the gain of each path $\alpha_\ell,\ell=1,\ldots,4$ follows a Gaussian distribution with mean zero and variance $\sigma_\alpha^2=1$. The AoAs/AoDs are sampled from a uniform distribution $\{\theta_k,\phi_k\}\sim \mathcal{U}(-\pi/2,\pi/2)$. Further, we assume the reciprocity mismatch gains follow a log-normal distribution, i.e. $\{\ln|t_{i,n}|,\ln|r_{i,n}|,\ln|t_{i,n}'|,\ln|r_{i,n}'|\}\sim \mathcal{N}(0,\sigma), i\in\{1,2\}, n=1\ldots N$, for standard deviation σ . Similarly, the phase of the mismatch parameters follows a uniform distribution $\{\angle t_{i,n},\angle r_{i,n},\angle t_{i,n}',\angle r_{i,n}'\}\sim \mathcal{U}(-\pi/16,\pi/16)$. Our tests are carried out on a server with an Intel i9 CPU at 2.3 GHz and 16 GBs of main memory.

B. Reciprocity Calibration between Two nodes

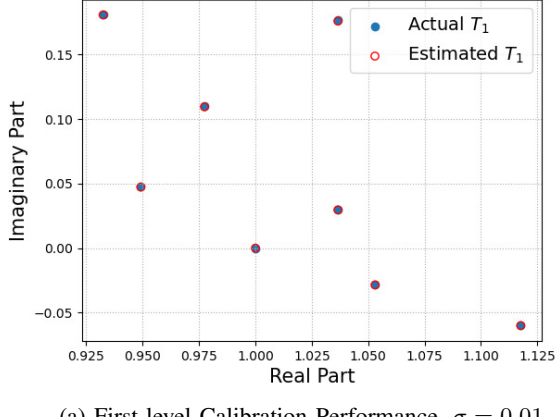
In this experiment we implement the calibration process described in sections III-A and III-B under different circumstances. Fig. 2(a, b) depict the normalized mean-square error

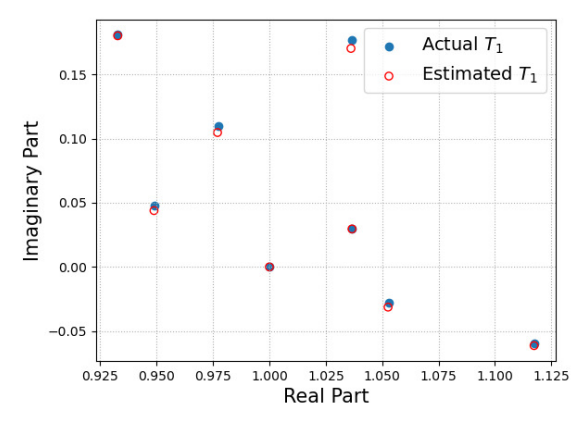
(NMSE) resulted from the calibration technique in estimating each of the calibration matrices for the digital and analog RF chains, versus the transmission noise variance, respectively. The actual and estimated calibration matrices are normalized with respect to the first element of the matrix to ignore the constant scaling factor in calculating the NMSE. We observe that in both steps, as the number of antennas per AP increases the NMSE curves are shifted downwards (NMSE improved by a factor of 1000), as there will be more observations which allow for making a more precise estimate of the calibration matrices.

Fig. 3 provides a visualization of the effectiveness of our proposed calibration approach under various noise variances. In Fig. 3, we consider M=32 antenna elements and N=8 digital RF chains at each AP. The scatter plots in Fig. 3(a,b) show the performance of the first step of the calibration process when estimating the calibration matrix T_1 for $\sigma=0.01$ and $\sigma=0.1$, respectively. It is observed that, in either case, the calibration parameters are obtained with high accuracy and as the noise variance gets smaller the estimation error reduces. In the second step of the calibration, one is interested in $R_2T_2^{-1}$ instead of the calibration matrices R_2 and T_2 itself. Fig. 3(c,d) presents similar results for the second step of the calibration.

V. CONCLUSIONS

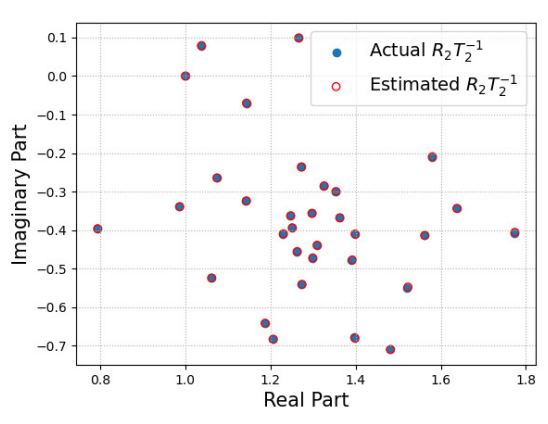
We presented a two-step approach for reciprocity calibration comprised of a first step for the first-level calibration of the mismatch related to the digital RF chains and a second step corresponding to the second-level calibration which builds on the results obtained for the first-level parameters. At each step, the channel reciprocity calibration is formulated as a least-square optimization problem that is efficiently solved by conventional methods. We verified the effectiveness of our calibration technique by means of numerical experiments. Simultaneous calibration of more than two APs for co-operative beamforming, together with joint calibration and synchronization of APs in a distributed MIMO system is among the future directions of our research.

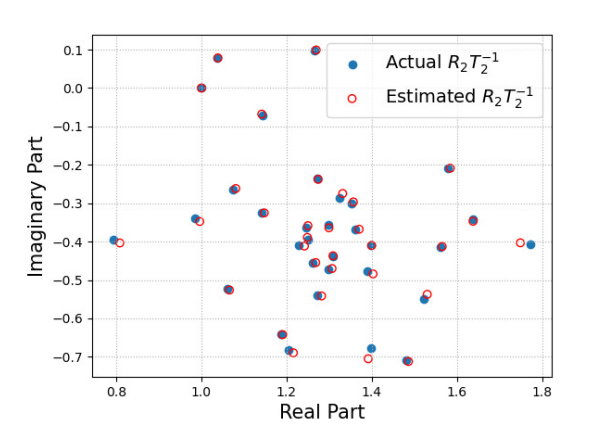




(a) First-level Calibration Performance, $\sigma = 0.01$.







(c) Second-level Calibration Performance, $\sigma = 0.01$

(d) Second-level Calibration Performance, $\sigma = 0.1$

Fig. 3: Channel Reciprocity Calibration Scheme Performance

REFERENCES

- [1] N. Torkzaban, M. A. Amir Khojastepour, and J. S. Baras, "Codebook design for composite beamforming in next-generation mmwave systems," in 2022 IEEE Wireless Communications and Networking Conference (WCNC), 2022, pp. 1545-1550.
- [2] N. Torkzaban and M. A. A. Khojastepour, "Codebook design for hybrid beamforming in 5g systems," in ICC 2022 - IEEE International Conference on Communications, 2022, pp. 1391-1396.
- [3] G. Interdonato, E. Björnson, H. Quoc Ngo, P. Frenger, and E. G. Larsson, "Ubiquitous cell-free massive mimo communications," EURASIP Journal on Wireless Comm. and Networking, vol. 2019, no. 1, pp. 1-13, 2019.
- [4] X. Wei, Y. Jiang, X. Wang, and C. Shen, "Tx-rx reciprocity calibration for hybrid massive mimo systems," IEEE Wireless Communications Letters, vol. 11, no. 2, pp. 431-435, 2022.
- J. Vieira and E. G. Larsson, "Reciprocity calibration of distributed massive mimo access points for coherent operation," in 2021 IEEE 32nd Annual International Symposium on Personal, Indoor and Mobile Radio Communications (PIMRC), 2021, pp. 783-787.
- [6] Y.-S. Yang, W.-C. Huang, C.-P. Li, H.-J. Li, and G. L. Stüber, "A low-complexity transceiver structure with multiple cfos compensation for ofdm-based coordinated multi-point systems," IEEE Transactions on Communications, vol. 63, no. 7, pp. 2658-2670, 2015.
- [7] F. Kaltenberger, H. Jiang, M. Guillaud, and R. Knopp, "Relative channel reciprocity calibration in mimo/tdd systems," in 2010 Future Network & Mobile Summit, 2010, pp. 1-10.
- [8] C. Shepard, H. Yu, N. Anand, E. Li, T. Marzetta, R. Yang, and L. Zhong, "Argos: Practical many-antenna base stations," in Proceedings of the 18th Annual International Conference on Mobile Computing and

- Networking, ser. Mobicom '12. New York, NY, USA: Association for Computing Machinery, 2012, p. 53-64. [Online]. Available: https://doi.org/10.1145/2348543.2348553
- J. Vieira, F. Rusek, and F. Tufvesson, "Reciprocity calibration methods for massive mimo based on antenna coupling," in 2014 IEEE Global Communications Conference, 2014, pp. 3708-3712.
- [10] R. Rogalin, O. Y. Bursalioglu, H. Papadopoulos, G. Caire, A. F. Molisch, A. Michaloliakos, V. Balan, and K. Psounis, "Scalable synchronization and reciprocity calibration for distributed multiuser mimo," IEEE Transactions on Wireless Communications, vol. 13, no. 4, pp. 1815-1831, 2014.
- J. Vieira, F. Rusek, O. Edfors, S. Malkowsky, L. Liu, and F. Tufvesson, "Reciprocity calibration for massive mimo: Proposal, modeling, and validation," IEEE Tran. on Wireless Comm., vol. 16, no. 5, pp. 3042-3056, 2017.
- [12] X. Jiang and F. Kaltenberger, "Channel reciprocity calibration in tdd hybrid beamforming massive mimo systems," IEEE Journal of Selected Topics in Signal Processing, vol. 12, no. 3, pp. 422-431, 2018.
- X. Wei, Y. Jiang, Q. Liu, and X. Wang, "Calibration of phase shifter network for hybrid beamforming in mmwave massive mimo systems," IEEE Transactions on Signal Processing, vol. 68, pp. 2302-2315, 2020.
- [14] R. Nie, L. Chen, Y. Chen, and W. Wang, "Hierarchical-absolute reciprocity calibration for millimeter-wave hybrid beamforming systems," 2022. [Online]. Available: https://arxiv.org/abs/2204.06705
- X. Jiang, M. vCirkić, F. Kaltenberger, E. G. Larsson, L. Deneire, and R. Knopp, "Mimo-tdd reciprocity under hardware imbalances: Experimental results," in 2015 IEEE International Conference on Communications (ICC), 2015, pp. 4949-4953.